EasyChair Preprint

№ 2090

# Mitigating Fluctuations of Wind Power Generation Using Superconducting Magnetic Energy Storage: a Passivity-Based Approach

Walter Gil-González, Alejandro Garces and Oscar Danilo Montoya



December 4, 2019

# Mitigating fluctuations of wind power generation using superconducting magnetic energy storage: a passivity-based approach

Walter Gil-González and Alejandro Garcés
*Programa de Ingeniería Eléctrica*
*Universidad Tecnológica de Pereira*
Pereira, Colombia
Email: {wjgil,alejandro.garces}@utp.edu.co

Oscar Danilo Montoya
*Programa de Ingeniería Eléctrica*
*Universidad Tecnológica de Bolivar*
Cartegana, Colombia
Email: o.d.montoyagiraldo@ieee.org

***Abstract*—This paper presents the control of the active and reactive power of a superconducting magnetic energy storage (SMES) system for compensating fluctuations of a power system with high penetration of wind energy during extreme scenarios of wind gusts. The wind energy conversion system (WECS) is a Type-A turbine with squirrel cage induction generator (SCIG) and a capacitor bank. A passivity-based proportional-integral control (PI-PBC) is used that controls the power transfer of the SMES system to the power grid. The proposed controller is designed with two main objectives: First, to deliver (or absorb) a suitable active power to (or from) the power system, and second, to regulate the voltage of the WECS. The proposed PI-PBC guarantees asymptotically stability in closed-loop and exploits the advantages of the proportional-integral (PI) actions. Also, it presents a superior performance when it is compared to a conventional PI controller and a proportional feedback linearization controller. Simulation results carried-out in MATLAB/SIMULINK demonstrate the advantages of the proposed methodology.**

## I. Introduction

Wind energy has shown significant growth worldwide because the wind is an available environmental-friendly resource. [1]. The penetration of wind energy has been mounting each year. In 2016, global wind power capacity increased in a 54,642 MW (12.5%) compared to the previous year [2]. This increase has been in distribution and transmission power systems.

Most of the wind energy conversion systems (WECS) uses power electronics for the integration of the resource to the grid. However, near $15\%$ of wind turbines are fixed-speed squirrel cage induction generators (SCIGs) because they are a simple, economical, profitable, and robust technology [3]. Nevertheless, these machines present two problems. First, when extreme wind gusts are presented, the generated power will have fluctuations which are not recommended for the power system. Second, the SCIG absorbs reactive power from the network because the induction machine requires magnetization. The former is usually avoided by disconnection of the generator whereas the later problem is compensated with parallel capacitors in terminals of the SCIGs [4].

One of the main problems of wind energy is the high variability of the speed of the wind, and for that reason, the wind is considered an intermittent and unpredictable resource [5], [6]. This makes output power difficult to predict and generates problems on the control and operation of the entire grid [7]. A fast-response energy reserve could be required to support power oscillation at high levels of wind energy penetration[8]. One of the most used forms to compensate power fluctuations is to use energy storage systems such as battery storage system [9], flywheel [10], and/or superconducting magnetic energy storage system (SMES) [11], [12]. The SMES systems have great the attention for this application due to their fast response, high energy storage efficiency (an efficiency around 95%) and, particularly the large amounts of discharge power during small periods [13].

The SMES system is a superconducting coil which maintains in a superconducting state due to the cryogenic cooler system and cryostat/vacuum vessel [14]. This system stores energy in the form of the magnetic field because of the flow of direct current in the coil. Besides, a SMES system requires power electronic interfaces to be integrated into the power systems. Typically, there are two major configurations employed for the SMES system, which are pulse-width modulated current source converter (PMW-CSC) and pulse-width-modulated voltage source converter (PWM-VSC) [15]. However, a PWM-CSC presents constructive costs a least $73\%$ higher than a PWM-VSC [5]. Besides, the PWM-CSC switches have commutation frequencies around 1 kHz, while the PWM-VSC switches permit commutation frequencies from 2 kHz to 20 kHz, which is a clear advantage in comparison to a PWM-CSC connection [5].

Several works investigating the use of the SMES system to WECS have studied. In [16] and [17], it is proposed a methodology that improves the transient stability of a multi-machines system connected to DFIG using the SMES system. In [18] shows small and slow power fluctuations that can be attenuated by the SMES system. In [19] employs the SMES system to reduce frequency fluctuations of isolated power system a with wind farm. Also, the SMES system

has been employed to regulate frequency in power systems with dynamic participation wind farm [20]. Some studies to enhance the dynamic performance of wind turbines during voltage sag/well suppression in the distribution system employ the SMES system [21]. Applications using the SMES system to improve the transient stability or the low-voltage-ride-through (LVRT) the capability of wind generators are shown in [22], [21] and in [23], respectively. Nevertheless, an exhaustive search of the relevant literature produced there is only one approach where smoothing power fluctuation of the wind farm during extreme wind speed gusts have been mitigated with a SMES system which was presented in [5]. That work employs a classical PI controller over VSC and a fuzzy logic controller about dc-dc chopper; however, these controllers do not guarantee stability in closed-loop.

This article proposes a passivity-based PI control, which guarantees structural stability properties in closed-loop from the non-linear point of view, and at the same time maintains the advantages of PI controllers in terms of robustness and straight forward implementation. The proposed methodology reduces power and voltage fluctuations of a grid-connected to fixed-speed WECS during extreme wind gust scenarios. The proposed controller focuses on controlling the active and reactive power of the SMES system and thus determines its charging/discharging cycles in order to alleviate the power oscillations generated by WECS; at the same time, it regulates the voltage profile at the point of common coupling. The PI passivity-based control (PI-PBC) is compared to a classical PI controller and a proportional feedback linearization controller where PI-PBC presents better performance than these two controllers. The proposed controller exploits the port-Hamiltonian (pH) structure of the SMES system in open-loop, allowing global asymptotical stability in closed-loop, which maintain a passive structure.

The rest of this paper is organized as follows: in Section II the dynamical model of a SMES system integrated to the grid with a VSC and the dc-dc chopper is shown; in Section III the general theory about passivity-based PI control is presented as well as stability analysis and controller design for the SMES system. In Section IV test system, simulating scenarios and results are widely discussed. Finally, the conclusions are given in Section V.

## II. SMES SYSTEM INTEGRATED WITH A VSC

The SMES system connected to the power system with a VSC is illustrated in Fig 1. This system has two converters: a dc-dc chopper and a two-level VSC. These converters are interconnected through of a common dc-link capacitor. Usually, the Gate Bipolar Transistor (IGBT) are employed as switch due to its high efficiency and fast switching characteristics [5].

The dynamic model in $abc$ reference frame presented in (1) is gotten applying the Kirchhoff's second law at the ac side of the VSC, the Tellegen's theorem to obtain the active power

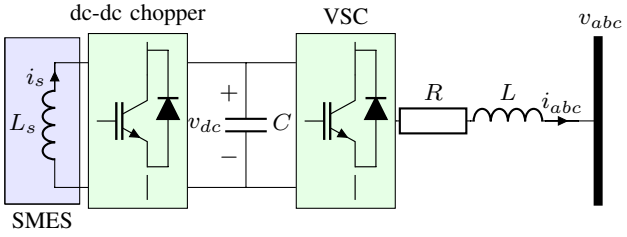


Fig. 1. The structure of a SMES system with a VSC

interchanged between the power system and the SMES system, and the Kirchhoff's first law at the SMES system.

$$\begin{aligned} L\frac{d}{dt}i_k &= -Ri_k + v_k - e_k, \\ Cv_{dc}\frac{d}{dt}v_{dc} &= (2D-1)v_{dc}i_s - \sum v_k i_k, \\ L_s\frac{d}{dt}i_s &= -(2D-1)v_{dc} \\ \forall k &\in \{a,b,c\}, \end{aligned} \tag{1}$$

where $R$ and $L$ denote the resistive and inductance parameters of the transformer, respectively. $i_k$ are currents that flow through of the transformer, $e_k$ and $v_k$ depict the ac voltage of the main grid and the output ac voltage of the VSC, respectively. $C$ is the dc-link capacitor of the VSC and its voltage is $v_{dc}$. $i_s$ is the current delivered (or absorbed) by the SMES system and $L_s$ is its inductance. $D$ represents the duty cycle of dc-dc chopper [24].

Observe that if $D > 0.5$, the SMES system will deliver energy into the power system, and when $D < 0.5$, the SMES system will absorb energy from the power system.

The duty cycle $D$ and the voltages $v_k$ can be written as,

$$\begin{aligned} v_k &= v_{dc}m_k \ \forall k \in \{a,b,c\}, \\ D &= \frac{m_s - 1}{2}, \end{aligned} \tag{2}$$

where $m_k, m_s \in [-1, 1]$ are the modulation indexes of the VSC and dc-dc chopper, respectively.

Dynamic model shown in (1) can be rewritten in the $dq$ reference frame, using the invariant power Park's transformation, as follows:

$$\begin{aligned} L\frac{d}{dt}i_d &= -Ri_d - \omega Li_q + m_d v_{dc} - e_d, \\ L\frac{d}{dt}i_q &= -Ri_q + \omega Li_d + m_q v_{dc} - e_q, \\ C\frac{d}{dt}v_{dc} &= m_s i_s - m_d i_d - m_q i_q, \\ L_s\frac{d}{dt}i_s &= -m_s v_{dc}, \end{aligned} \tag{3}$$

where $\omega$ is the grid angular electrical frequency and is obtained using a classical phase-locked loop (PLL) [25].

The dynamical system (3) can be represented as a port-Hamiltonian system as follows:

$$Q\dot{x} = \left( J_o + \sum_{i=1}^{3} J_i u_i - R \right) x + d, \tag{4}$$

where $x = [i_d, i_q, v_{dc}, i_s]^T$, $d = [-e_d, -e_q, 0, 0]^T$, $u = [m_d, m_q, m_s]^T$, $Q = \mathbf{diag}\{L, L, C, L_s\}$, $R = \mathbf{diag}\{R, R, 0, 0\}$, while

$$J_o = \begin{bmatrix} 0 & -\omega L & 0 & 0 \\ \omega L & 0 & 0 & 0 \\ 0 & 0 & 0 & 0 \\ 0 & 0 & 0 & 0 \end{bmatrix}, \quad J_1 = \begin{bmatrix} 0 & 0 & 1 & 0 \\ 0 & 0 & 0 & 0 \\ -1 & 0 & 0 & 0 \\ 0 & 0 & 0 & 0 \end{bmatrix},$$

$$J_2 = \begin{bmatrix} 0 & 0 & 0 & 0 \\ 0 & 0 & 1 & 0 \\ 0 & -1 & 0 & 0 \\ 0 & 0 & 0 & 0 \end{bmatrix}, \quad J_3 = \begin{bmatrix} 0 & 0 & 0 & 0 \\ 0 & 0 & 0 & 0 \\ 0 & 0 & 0 & 1 \\ 0 & 0 & -1 & 0 \end{bmatrix},$$

where $x$ is the vector of the state variables and $d$ corresponds to the vector of the external inputs and $u$ is the vector input control. The matrix $Q$ is known as inertia matrix, $J$ are the interconnection matrices which are knew-asymmetric and the matrix $R$ is known as damping matrix.

## III. Passivity-based PI control

The PBC theory is a control technique adequate and efficient when is applied to dynamical systems with a port-Hamiltonian structure [26], [27]. This theory guarantees stability conditions for affine and non-affine systems in the sense of Lyapunov for the closed-loop dynamical system [27], [13]. In case of non-affine systems, as it is the case of the dynamical model presented in (3), the classical PBC and PI passive techniques are more appropriated control approach to design the controller [28].

Let $x_\star$ is an admissible trajectory, i.e., $x_\star$ exists, is differentiable, bounded and satisfies

$$Q\dot{x}_\star = \left( J_o + \sum_{i=1}^{3} J_i u_{i\star} - R \right) x_\star + d, \tag{5}$$

and it is generated by some $u_\star$ bounded. Finally, $x_\star$ is not reached if does not exist any $u_\star$ that generates it.

Let us consider the dynamical system presented in (6) as function of the error dynamics, i.e.,, $\tilde{x} = x - x_\star$ and $\tilde{u} = u - u_\star$, which is obtained by substituting these errors on (4),

$$Q\left(\dot{\tilde{x}} + \dot{x}_\star\right) = \left( J_o + \sum_{i=1}^{3} J_i \left(\tilde{u}_i + u_{i\star}\right) - R \right) \left(\tilde{x} + x_\star\right) + d, \tag{6}$$

and substituting (5) in (6) is achieved,

$$Q\dot{\tilde{x}} = \left( J_o + \sum_{i=1}^{3} J_i u_i - R \right) \tilde{x} + \sum_{i=1}^{3} J_i x_\star \tilde{u}_i. \tag{7}$$

The error dynamics model presented in (7) for the output $y = \mathcal{C}x$, where

$$\mathcal{C} = - \begin{bmatrix} x_\star^T J_1 \\ x_\star^T J_2 \\ x_\star^T J_3 \end{bmatrix} \tag{8}$$

is passive, if fulfills the dissipation inequality $\dot{H} \leq \tilde{y}^T \tilde{u}$, where $\tilde{y} = y - y_\star$, $y_\star = \mathcal{C}x_\star$, and a storage function as

$$H(\tilde{x}) = \frac{1}{2}\tilde{x}^T Q \tilde{x}. \tag{9}$$

Taking the temporal derivative of $H$, the following result is achieved:

$$\begin{aligned} \dot{H}(\tilde{x}) &= \tilde{x}^T Q \dot{\tilde{x}} \\ &= \tilde{x}^T \left( \left( J_o + \sum_{i=1}^{3} J_i u_i - R \right) \tilde{x} + \sum_{i=1}^{3} J_i x_\star \tilde{u}_i \right) \\ &= -\tilde{x}^T R \tilde{x} + \tilde{x}^T \sum_{i=1}^{3} J_i x_\star \tilde{u}_i \\ &\leq \tilde{x}^T \sum_{i=1}^{3} J_i x_\star \tilde{u}_i = \tilde{y}^T \tilde{u}, \end{aligned} \tag{10}$$

this demonstrates that the system presented in (7) is passive.

Now, let us consider that pH system given in (4) has an $x_\star$ in closed-loop with the following PI controller

$$\begin{aligned} \dot{z} &= -\tilde{y}, \\ \tilde{u} &= -K_p \tilde{y} + K_i z, \end{aligned} \tag{11}$$

where $K_p = K_p^T \succ 0$, $K_i = K_i^T \succ 0$. Additionally, the trajectories of the closed-loop system are bounded and such that

$$\lim_{t \longrightarrow \infty} \mathcal{C}\tilde{x}(t) = 0 \Rightarrow \lim_{t \longrightarrow \infty} x(t) = x_\star \tag{12}$$

### A. Stability Analysis

Let us define the Lyapunov function candidate in (13) to prove the stability of the dynamical system given by (7).

$$V(\tilde{x}, z) = H + \frac{1}{2} z^T K_i z. \tag{13}$$

Observe that $V(\tilde{x}, z) > 0 \ \forall x \neq x_\star \in \mathbb{R}^n$ and $V(0, 0) = 0 \ \forall x = x_\star$. The time derivative of the $V(\tilde{x}, z)$ is

$$\dot{V}(\tilde{x}, z) = \dot{H} + z^T K_i \dot{z} \tag{14}$$

$$= -\tilde{x}^T R \tilde{x} + \tilde{y}^T \tilde{u} + z^T K_i (-\tilde{y}) \tag{15}$$

$$\leq \tilde{y}^T \tilde{u} + (\tilde{u} + K_p \tilde{y})^T (-\tilde{y}) = -\tilde{y}^T K_p \tilde{y} \leq 0 \tag{16}$$

this proves that the dynamical system is stable, which implies that (12) is satisfied. Moreover, if

$$rank \begin{bmatrix} \mathcal{C} \\ R^{\frac{1}{2}} \end{bmatrix} = n,$$

then the dynamical system given by (7) is globally asymptotically stable [13], with $R^{\frac{1}{2}}$ the square root of $R$.

### B. Controller Design for the SMES system

The controller design for the SMES system is based on Passivity-based PI control presented in the above subsection. The output $y$ that guarantees that the pH system shown in (7) is passive, it is given in (17).

$$y = \begin{bmatrix} i_d v_{dc}^\star - i_d^\star v_{dc} \\ i_q v_{dc}^\star - i_q^\star v_{dc} \\ i_s^\star v_{dc} - i_s v_{dc}^\star \end{bmatrix}, \tag{17}$$

and, globally asymptotically stable is proved by means of the matrix

$$\mathcal{C} = \begin{bmatrix} v_{dc}^\star & 0 & -i_d^\star & 0 \\ 0 & v_{dc}^\star & -i_q^\star & 0 \\ 0 & 0 & i_s^\star & -v_{dc}^\star \\ \frac{\sqrt{R}}{2} & 0 & 0 & 0 \\ 0 & \frac{\sqrt{R}}{2} & 0 & 0 \\ 0 & 0 & 0 & 0 \\ 0 & 0 & 0 & 0 \end{bmatrix},$$

the rank condition is satisfied if and only if $v_{dc}^\star \neq 0$ and $i_s^\star \neq 0$, which is presented in the operating mode of a VSC and a SMES system, since $v_{dc} > 0$ and $i_s > 0$.

Now, defining the reference values which depends on the control requirement of the SMES system, in this sense, the objectives of controlling in this paper are $v_{dc}$, $i_d$ and $i_q$. $v_{dc}^\star$ permits to control dc-link voltage on the capacitor $C$, i.e., $v_{dc}^\star = v_{dc}^{nom}$ and, $i_d\star$ and $i_q\star$ allow controlling the active and reactive power of the SMES system to the power system. $i_d^\star$ and $i_q^\star$ are selected, as follows,

$$\begin{aligned} i_d^\star &= \frac{e_d p^\star + e_q q^\star}{e_d^2 + e_q^2}, \\ i_q^\star &= \frac{e_q p^\star - e_d q^\star}{e_d^2 + e_q^2}, \end{aligned} \tag{18}$$

where $p^\star$ and $q^\star$ are the reference values of the active and reactive power, respectively.

From (5) are gotten $u_\star$ and the admissible trajectories with which the design of the controller is completed, as follows,

$$\begin{aligned} m_d^\star &= \frac{L\dot{i}_d^\star + L\omega i_q^\star + e_d + R i_d^\star}{v_{dc}^\star}, \\ m_q^\star &= \frac{L\dot{i}_q^\star - L\omega i_d^\star + e_q + R i_q^\star}{v_{dc}^\star}, \\ m_s^\star &= \frac{C\dot{v}_{dc}^\star + m_d^\star i_d^\star + m_q^\star i_q^\star}{i_s^\star}, \\ i_s^\star &= \frac{-1}{L_s}\int_0^t m_s^\star v_{dc}^\star dt. \end{aligned}$$

## IV. Test System, Simulation and Results

### A. Test system

Fig 2 depicts the test system used to demonstrate the compensation of fluctuations of the generated power and voltage of power systems connected to during the wind gusts scenarios

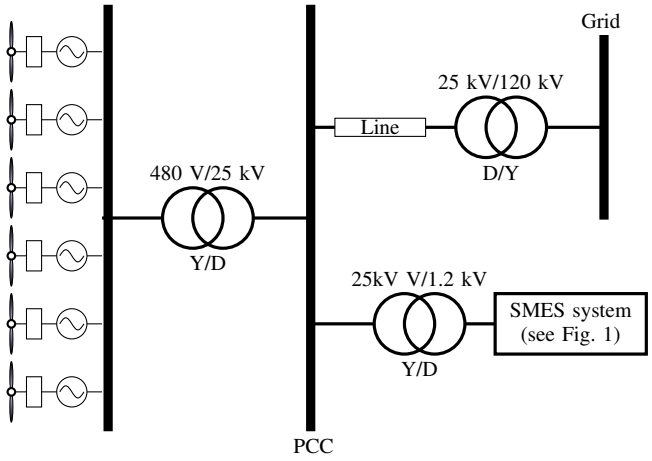


Fig. 2. WECS connected to the power system

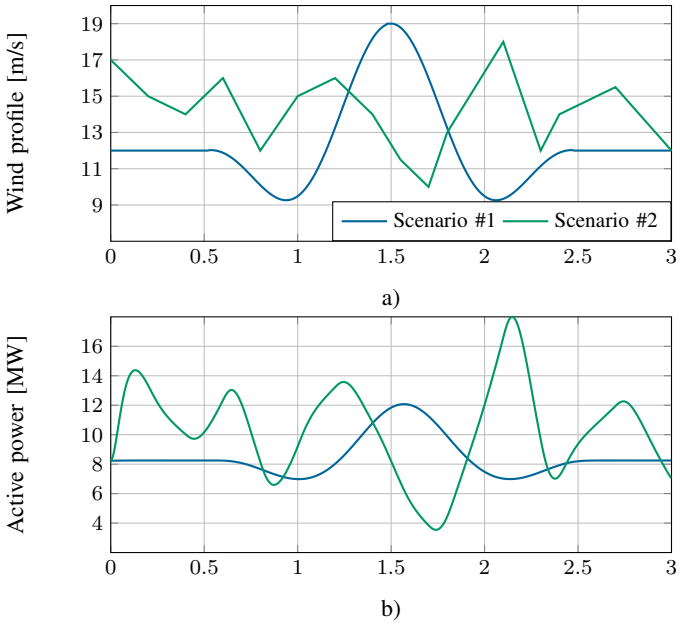


Fig. 3. Wind gust scenarios and the active power at PCC: a) proposed Scenario, and b) the active power generated by WECS

by the SMES system. The test system is composed of six SCIG wind turbine which are equipped with capacitor banks connected at each wind turbine low voltage bus to compensate the reactive power absorbed for them. Besides, SCIG wind turbine and the SMES system have installed at the point of common coupling (PCC) and all their parameters are given in [5].

### B. Simulation scenarios

To prove the performance and robustness of the proposed control two wind gust scenarios are considered (see Fig. 3a) [5]). The active powers generated by WECS each scenario are illustrated in same figure (see Fig. 3b)).

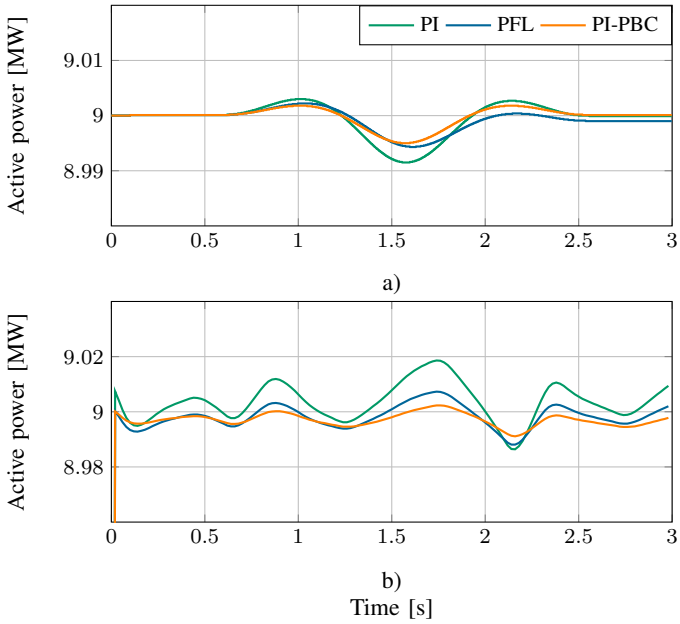


Fig. 4. Active energy at PCC to the grid during wind gusts: a) Scenario #1, and b) Scenario #2

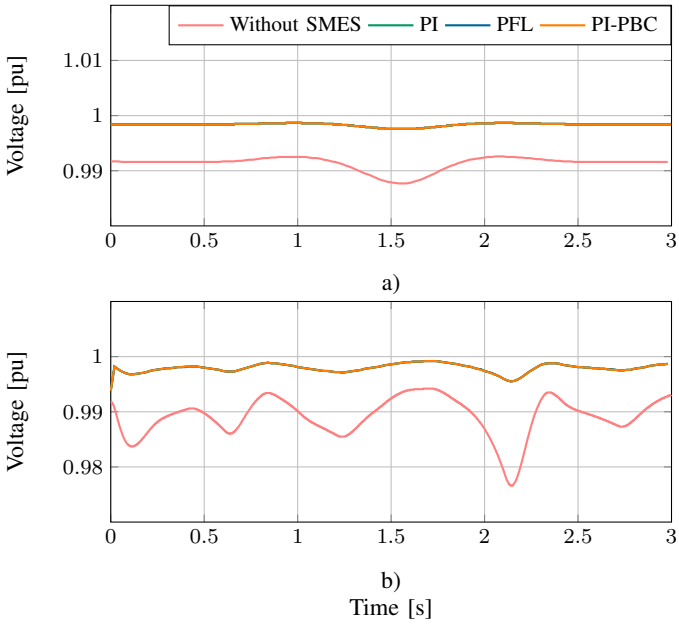


Fig. 5. Voltage profile of PCC during wind gusts: a) Scenario #1, and b) Scenario #2

Additionally, we consider two control objectives. The first objective is to maintain the active power of PCC in nominal power of the WECS, i.e., $P_{nom} = 9MW$. The second objective is to control voltage of PCC keeping on 1.0 pu. In order to fulfill with the proposed objectives, the reference values for the active and reactive power are defined, as follows

$$p^{\star} = P_{nom} - P_{wind},$$
$$q^{\star} = K(v_{pcc} - v_{\star}),$$

where $P_{wind}$ is the generated power of the the WECS and $K$ is a gain of the primary voltage control, which is $K = 10^9$.

It is considered that the SMES system has an initial charge of 50% of its maximum current [5]. Also, comparisons with the classical PI controller (PI) and proportional feedback linearization controller (PFL) presented in [6] are shown.

### C. Results

Two scenarios consider for the power system presented in Fig. 2 have been carried-out in the MATLAB/Simulink software.

Fig. 4 shows the active power at PCC to the grid during wind gusts when the SMES system is connected. Observe that the fluctuations of the active power are compensated in an effective form. i.e., to keep $P_{nom} = 9MW$ at PCC. This demonstrates that the SMES system alleviates the power fluctuations generated by WECS due to the rapid variations of the wind during extreme wind gusts.

Although that the three controllers keep the active power on the proposed objective, the proposed controller has a better performance because is able to follow the desired references with fewer power oscillations than the other two controllers employed.

In Fig. 5 illustrates the voltage profile of the PCC during wind gust without and with the SMES system. Note that the voltage profile has drops from 1.0 pu to 0.976 pu when the SMES system is not used (see Fig. 5b)). When the SMES system is employed the voltage profile maintains on 1.0 pu for all controllers employed.

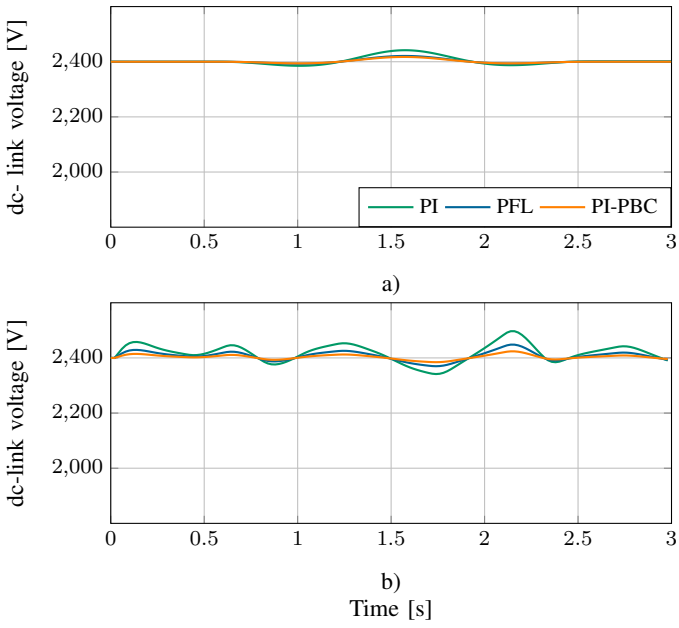


Fig. 6. Response of dc-link voltage during wind gusts: a) Scenario #1, and b) Scenario #2

Fig. 6 depicts dc-link voltage during wind gusts. Observe

that the controllers employed the voltage on dc-link is approximately constant at 2400 V over different modes of the SMES system. Nevertheless, PI-PBC continues to perform better than the PI and PFL controllers. This enhanced performance of the PI-PBC is due to $u_\star$ allows reaching the desired reference faster and its PI controller regulates behavior around of desired operating point [29].

## V. Conclusions

This paper showed a control strategy of the active and reactive power of a SMES system to compensate the power and voltage fluctuations of a power system connected to WECS during extreme scenarios of wind gusts. The SMES system proved to be a good option to support power oscillations generated by wind power when high and fast of wind are presented. This is due to the characteristic of the large amounts of discharge power for small periods of time that the SMES system has.

A PI-PBC to integrate superconducting coils in the power system guaranteeing global asymptotically operating conditions under closed-loop via passivity formulation was presented. The PI-PBC exploits the advantages of a classical proportional-integral actions under passivity-based representation showing superior performance when is compared to a conventional PI design and a PFL controller.

## Financial support

This work was partially supported by the National Scholarship Program Doctorates of the Administrative Department of Science, Technology and Innovation of Colombia (COLCIENCIAS), by calling contest 727-2015.

## References

[1] L. Freris and D. Infield, *Renewable energy in power systems*. John Wiley & Sons, 2008.

[2] G. W. E. Council, "Global wind 2015 report: Annual market update," *Global Wind Energy Council (GWEC), Brussels, Belgium*, 2017.

[3] M. Rahimi and M. Parniani, "Dynamic behavior and transient stability analysis of fixed speed wind turbines," *Renewable energy*, vol. 34, no. 12, pp. 2613–2624, 2009.

[4] G. M. Masters, *Renewable and efficient electric power systems*. John Wiley & Sons, 2013.

[5] M. M. Aly, M. Abdel-Akher, S. M. Said, and T. Senjyu, "A developed control strategy for mitigating wind power generation transients using superconducting magnetic energy storage with reactive power support," *International Journal of Electrical Power & Energy Systems*, vol. 83, pp. 485–494, 2016.

[6] O. D. Montoya, A. Garcés, and F. M. Serra, "DERs integration in microgrids using VSCs via proportional feedback linearization control: Supercapacitors and distributed generators," *J. Energy Storage*, vol. 16, pp. 250–258, 2018.

[7] M. Khalid and A. Savkin, "An optimal operation of wind energy storage system for frequency control based on model predictive control," *Renewable energy*, vol. 48, pp. 127–132, 2012.

[8] L. F. Grisales, A. Grajales, O. D. Montoya, R. A. Hincapie, M. Granada, and C. A. Castro, "Optimal location, sizing and operation of energy storage in distribution systems using multi-objective approach," *IEEE Latin America Transactions*, vol. 15, no. 6, pp. 1084–1090, 2017.

[9] B. D. Olaszi and J. Ladanyi, "Comparison of different discharge strategies of grid-connected residential pv systems with energy storage in perspective of optimal battery energy storage system sizing," *Renewable and Sustainable Energy Reviews*, vol. 75, pp. 710–718, 2017.

[10] F. Faraji, A. Majazi, K. Al-Haddad *et al.*, "A comprehensive review of flywheel energy storage system technology," *Renewable and Sustainable Energy Reviews*, vol. 67, pp. 477–490, 2017.

[11] W. Gil-González and O. D. Montoya, "Active and reactive power conditioning using SMES devices with PMW-CSC: A feedback nonlinear control approach," *Ain Shams Engineering Journal*, vol. 10, no. 2, pp. 369–378, 2019.

[12] O. D. Montoya, W. Gil-González, and A. Garces, "Control for EESS in Three–Phase Microgrids Under Time–Domain Reference Frame via PBC Theory," *IEEE Transactions on Circuits and Systems II: Express Briefs*, 2019.

[13] W. Gil, O. D. Montoya, A. Garces *et al.*, "Direct power control of electrical energy storage systems: A passivity-based PI approach," *Electric Power Systems Research*, vol. 175, p. 105885, 2019.

[14] S. Wang and J. Jin, "Design and Analysis of a Fuzzy Logic Controlled SMES System," *IEEE Trans. Appl. Supercond.*, vol. 24, no. 5, pp. 1–5, Oct 2014.

[15] W. J. Gil-González, A. Garcés, and A. Escobar, "A generalized model and control for supermagnetic and supercapacitor energy storage," *Ingeniería y Ciencia*, vol. 13, no. 26, pp. 147–171, 2017.

[16] W.-K. Ham, S.-W. Hwang, and J.-H. Kim, "Active and reactive power control model of superconducting magnetic energy storage (SMES) for the improvement of power system stability," *Journal of Electrical Engineering and Technology*, vol. 3, no. 1, pp. 1–7, 2008.

[17] S. M. Said, M. M. Aly, and M. Abdel-Akher, "Application of Superconducting Magnetic Energy Storage (SMES) to Improve Transient Stability of Multi-Machine System with Wind Power Penetration," in *16th International Middle-East Power Systems Conference*, 2014, pp. 23–25.

[18] C. Liu, C. Hu, X. Li, Y. Chen, M. Chen, and D. Xu, "Applying SMES to smooth short-term power fluctuations in wind farms," in *Industrial Electronics, 2008. IECON 2008. 34th Annual Conference of IEEE*. IEEE, 2008, pp. 3352–3357.

[19] W. Xian, W. Yuan, Y. Yan, and T. Coombs, "Minimize frequency fluctuations of isolated power system with wind farm by using superconducting magnetic energy storage," in *Power Electronics and Drive Systems, 2009. PEDS 2009. International Conference on*. IEEE, 2009, pp. 1329–1332.

[20] P. Bhatt, S. Ghoshal, and R. Roy, "Coordinated control of TCPS and SMES for frequency regulation of interconnected restructured power systems with dynamic participation from DFIG based wind farm," *Renewable Energy*, vol. 40, no. 1, pp. 40–50, 2012.

[21] A. S. Yunus, M. A. Masoum, and A. Abu-Siada, "Application of SMES to enhance the dynamic performance of DFIG during voltage sag and swell," *IEEE Trans. Appl. Supercond*, vol. 22, no. 4, pp. 5 702 009–5 702 009, 2012.

[22] T. Kinjo, T. Senjyu, N. Urasaki, and H. Fujita, "Terminal-voltage and output-power regulation of wind-turbine generator by series and parallel compensation using SMES," *IEE Proceedings-Generation, Transmission and Distribution*, vol. 153, no. 3, pp. 276–282, 2006.

[23] A. S. Yunus, A. Abu-Siada, and M. A. Masoum, "Improvement of LVRT capability of variable speed wind turbine generators using SMES unit," in *Innovative Smart Grid Technologies Asia (ISGT), 2011 IEEE PES*. IEEE, 2011, pp. 1–7.

[24] X. Lin and Y. Lei, "Coordinated Control Strategies for SMES-Battery Hybrid Energy Storage Systems," *IEEE Access*, vol. 5, pp. 23 452–23 465, 2017.

[25] S. Golestan, J. M. Guerrero, and J. C. Vasquez, "Three-phase PLLs: A review of recent advances," *IEEE Transactions on Power Electronics*, vol. 32, no. 3, pp. 1894–1907, 2017.

[26] O. D. Montoya, A. Garcés, and G. Espinosa-Pérez, "A generalized passivity-based control approach for power compensation in distribution systems using electrical energy storage systems," *J. Energy Storage*, vol. 16, pp. 259–268, 2018.

[27] R. Ortega, A. van der Schaft, B. Maschke, and G. Escobar, "Interconnection and damping assignment passivity-based control of port-controlled hamiltonian systems," *Automatica*, vol. 38, no. 4, pp. 585 – 596, 2002.

[28] M. Pérez, R. Ortega, and J. R. Espinoza, "Passivity-based PI control of switched power converters," *IEEE Trans. Control Syst. Technol.*, vol. 12, no. 6, pp. 881–890, 2004.

[29] S. Aranovskiy, R. Ortega, and R. Cisneros, "A robust PI passivity-based control of nonlinear systems and its application to temperature regulation," *International Journal of Robust and Nonlinear Control*, vol. 26, no. 10, pp. 2216–2231, 2016.